

## Self-Doped Polyphenylenes Containing Electron-Accepting Viologen Side Group

Isao Yamaguchi,\* Naotaka Mizoguchi, and Moriyuki Sato

*Department of Material Science, Faculty of Science and Engineering, Shimane University, 1060 Nishikawatsu, Matsue 690-8504, Japan*

*Received March 12, 2009; Revised Manuscript Received April 21, 2009*

**ABSTRACT:** Polyphenylenes (PPs) with  $\text{NH}_2$  side groups, namely, PFlu $\text{NH}_2$  and PPh $\text{NH}_2$ , were synthesized by the Pd-complex-catalyzed reaction of 2,5-dibromoaniline with 9,9-dihexylfluorene-2,7-diboronic acid bis(1,3-propanediol) ester and 2,6-dioctyloxybenzene-1,4-diboronic acid. The reaction of PFlu $\text{NH}_2$  and PPh $\text{NH}_2$  with 1-alkyl-1'-(2,4-dinitrophenyl)-4,4'-bipyridinium dichloride (alkyl = ethyl and *n*-hexyl) eliminated 2,4-dinitroaniline to yield PPs with viologen (1,1'-disubstituted 4,4'-bipyridinium dications) side groups, namely, PFluBPyHex, PFluBPyEt, and PPhBPyEt. The UV–vis spectra of PFluBPyHex, PFluBPyEt, and PPhBPyEt showed absorptions due to the viologen radical cation that was formed under nitrogen by the electron transfer from the polymer backbone to the viologen moiety. In contrast to photoluminescent PFlu $\text{NH}_2$  and PPh $\text{NH}_2$ , PFluBPyHex, PFluBPyEt, and PPhBPyEt showed no photoluminescence because the viologen contained within them acted as a quencher. The ESR spectra of PFluBPyEt and PPhBPyEt confirmed the generation of the viologen radical. Cyclic voltammetry measurements suggested that an electrochemical reduction of the viologen moiety and oxidation of the polymer backbone within PFluBPyEt and PPhBPyEt. Furthermore, this reaction was accompanied by electrochromism. The electric conductivities ( $\sigma$ ) of the pellets molded from PFluBPyEt and PPhBPyEt were  $6.4 \times 10^{-6}$  and  $1.1 \times 10^{-6} \text{ S cm}^{-1}$ , respectively; these  $\sigma$  values were higher than those of PFlu $\text{NH}_2$  and PPh $\text{NH}_2$  ( $\sigma < 10^{-8} \text{ S cm}^{-1}$ , respectively) due to the self-doping in PFluBPyEt and PPhBPyEt.

### Introduction

Polyphenylenes (PPs) have been extensively studied because they can be useful materials for the development of electronic and photoelectronic devices.<sup>1</sup> It is known that PPs can undergo a reductive (n-type) or an oxidative (p-type) of doping; the p-doping of PPs effectively converts them into conducting materials.<sup>1,2</sup> In addition to conventional doping methods, several other methods have been applied for the p-doping of PPs. For example, the introduction of sulfonic acid groups in the polymer chain has been used for the self-doping of PPs.<sup>3</sup> However, this process is highly pH-dependent, and in order to achieve a substantial increase in conductivity, an acid solution with a pH of less than 4 is necessary. This doping condition presents a harsh and corrosive environment for industrial applications. As a means of finding a milder environment for doping, we explored the use of viologen (1,1'-disubstituted 4,4'-bipyridinium dications), a well-known redox agent, to convert PPs from an insulating to a conducting state. The self-doping nature of PPs that contain a viologen side group can be explained by the electron transfer from the polymer backbone to the viologen. It has been reported that polythiophenes with a viologen side group cause the electron transfer from the thiophene unit to the viologen moiety.<sup>4</sup> Recently, we have reported the polyanilines with a viologen side chain.<sup>5</sup> The polyaniline self-doping occurred at  $1 \leq \text{pH} \leq 10$ , which is noteworthy when we consider that sulfonated polyaniline became an insulator at pH above 7.<sup>6</sup> However, the above-mentioned conducting polymers had nonconjugated alkyl or sulfo spacing groups between the polymer backbone and the viologen moiety.  $\pi$ -Conjugated polymers containing the viologen moiety without the spacing group could easily cause an electron

transfer from the polymer backbone to the viologen moiety, leading to improved electric properties. To the best of our knowledge, however, there have been no studies on  $\pi$ -conjugated polymers containing the viologen moiety bonded to the polymer backbone without the spacing group. This appears to be due to difficulty associated with synthesizing  $\pi$ -conjugated polymers containing the viologen moiety bonded to the polymer backbone.

$\pi$ -Conjugated polymers with reactive functional groups have been attracting interest.<sup>7–16</sup> For example,  $\pi$ -conjugated polymers with a sulfo group,<sup>7–9</sup> a carboxylic group,<sup>10–13</sup> or a hydroxyl group<sup>14,15</sup> have been reported. However, there are a few reports on  $\pi$ -conjugated polymers with  $\text{NH}_2$  side group(s).<sup>16</sup> The reactive  $\text{NH}_2$  side group can be useful for the introduction of a viologen moiety at the side chain of PPs because the reaction between Zincke salts (highly electrophilic species formed by the reaction between a pyridine derivative and 1-chloro-2,4-dinitrobenzene) with primary amines yields pyridinium salts.<sup>17</sup> Recently, we have reported a Zincke salt, *N*-(2,4-dinitrophenyl)-4-(4-pyridyl)pyridinium chloride, which can be a starting material for the synthesis of PPs containing the viologen moiety.<sup>18</sup> An investigation of the chemical properties of the PPs containing the viologen moiety would facilitate a better understanding of the chemical properties of PPs and development of new conducting materials.

Amplified quenching of fluorescent conjugated polymers has also received considerable attention because of its potential for application in ultrasensitive chemo- and biosensors.<sup>19</sup> It is well-known that viologens induce a quenching effect on fluorescent  $\pi$ -conjugated polymers and aromatic compounds.<sup>19</sup> In this work, the fluorescent properties of PPs containing the viologen moiety and PPs in the presence of viologen were investigated. These data will allow us to better understand the quenching effect of viologen on PPs and facilitate the development of chemo- and biosensors.

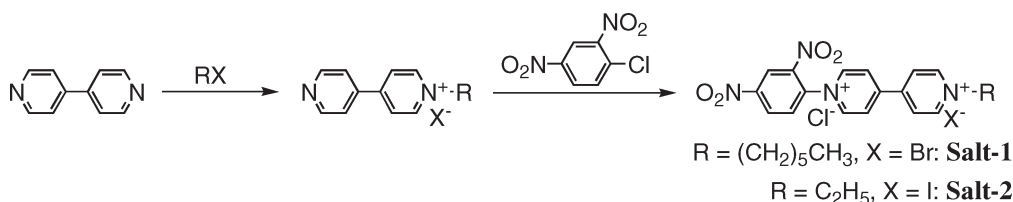
\*Corresponding author. E-mail: iyamaguchi@riko.shimane-u.ac.jp.

Table 1. Synthesis Results and Optical and Electrochemical Properties of Polymers

	yield (%)	$M_n^a$	$M_w^a$	$\eta_{sp}c^{-1}/dL\ g^{-1}$	absorption/nm	$\lambda_{em}/nm^h$	$K_{SV}/M^{-1}i$	oxidation potential/V <sup>j</sup>	reduction potential/V <sup>j</sup>			
									$E_{pc}(1)$	$E_{pc}(2)$	$E_{pa}(1)$	$E_{pa}(2)$
PFluNH <sub>2</sub>	98	20930	36090	0.26 <sup>c</sup>	361 <sup>f</sup>	422 (0.11)	$3.3 \times 10^2$	0.90, 1.60				
PPhNH <sub>2</sub>	88	4470	7980	0.10 <sup>c</sup>	340 <sup>f</sup>	411 (0.03)	$1.8 \times 10^3$	0.97, 1.61				
PFluBPyEt	87	— <sup>b</sup>	— <sup>b</sup>	1.56 <sup>d</sup>	366, 400, 570, 613, 665 <sup>g</sup>			1.53	−0.78	−1.23	−0.54	−1.02
PFluBPyHex	89	— <sup>b</sup>	— <sup>b</sup>	2.03 <sup>d</sup>	366, 400, 570, 613, 665 <sup>g</sup>			1.50	−0.59	1.06	−0.40	−0.80
PPhBPyEt	97	— <sup>b</sup>	— <sup>b</sup>	0.19 <sup>d</sup>	347, 403, 570, 609, 665 <sup>g</sup>			1.52	−0.68	−1.19	−0.48	−0.99
PFluPyPy	77	— <sup>b</sup>	— <sup>b</sup>	0.12 <sup>e</sup>	345 <sup>g</sup>			1.57	−0.86	−1.33	−0.64	−1.10
PFluPyPyEt-a	70	— <sup>b</sup>	— <sup>b</sup>	1.07 <sup>d</sup>	357, 400, 570, 623, 665 <sup>g</sup>							
PFluPyPyEt-b	85	— <sup>b</sup>	— <sup>b</sup>		357, 400, 570, 623, 665 <sup>g</sup>			1.46	−0.70	−1.10	−0.45	−0.86

<sup>a</sup> Determined by GPC (eluent = CHCl<sub>3</sub> vs polystyrene standards). <sup>b</sup> Not measured due to insolubility in the eluent. <sup>c</sup> Measured at the concentration of 0.10 g dL<sup>−1</sup> in CHCl<sub>3</sub> at 30 °C. <sup>d</sup> Measured at the concentration of 0.10 g dL<sup>−1</sup> in DMF at 30 °C. <sup>e</sup> Measured at the concentration of 0.10 g dL<sup>−1</sup> in DMSO at 30 °C. <sup>f</sup> In CHCl<sub>3</sub>. <sup>g</sup> In DMSO. <sup>h</sup> Photoluminescence (PL) peak in CHCl<sub>3</sub>. Quantum yields of PL were shown in parentheses. <sup>i</sup> Stern–Volmer constant. <sup>j</sup> Measured by cyclic voltammetry in a DMSO solution of [Et<sub>4</sub>N]BF<sub>4</sub> (0.10 M).

Scheme 1. Synthesis of 1-Alkyl-1'-2,4-dinitrophenyl-4,4'-bipyridinium Salts



Herein, we report the synthesis of PPs containing the viologen moiety and their optical, electrochemical, and thermal properties. In addition, we describe the synthesis of novel Zincke salts and model compounds, comparing their optical and electrochemical properties with those of PPs containing the viologen moiety.

## Results and Discussion

**Synthesis.** The introduction of the viologen side group in PPs was carried out by the reaction between Zincke salts and PPs with NH<sub>2</sub> groups. The new Zincke salts used in this study, Salt-1 and Salt-2, that were synthesized by the two-step *N*-alkyl and *N*-aryl reactions of 4,4'-bipyridyl (Scheme 1).

The Pd-complex-catalyzed polycondensation of 2,5-dibromoaniline with 9,9-dihexylfluorene-2,7-diboronic acid bis(1,3-propanediol) ester and 2,6-dioctyloxybenzene-1,4-diboronic acid resulted in 98% and 88% yields of polyphenylenes PFluNH<sub>2</sub> and PPhNH<sub>2</sub>, respectively, as shown in Scheme 2a. The reaction of Salt-1 and Salt-2 with PFluNH<sub>2</sub> and PPhNH<sub>2</sub> caused the elimination of 2,4-dinitroaniline and yielded polyphenylenes with the viologen moiety. PFluBPyHex, PFluBPyEt, and PPhBPyEt were produced in 89%, 87%, and 97% yields, respectively. The synthesis results are summarized in Table 1. The <sup>1</sup>H NMR spectra suggest that all the NH<sub>2</sub> groups of PFluNH<sub>2</sub> were converted into the viologen moiety in PFluBPyHex and PFluBPyEt (Scheme 2b). However, the <sup>1</sup>H NMR spectrum of PPhBPyEt confirmed that this polyphenylene contained the viologen and unreacted units in a 0.52:0.48 molar ratio (Scheme 2c); the lower content of the viologen moiety in PPhBPyEt was apparently due to the steric hindrance of the OC<sub>8</sub>H<sub>17</sub> side groups.

The reaction of PFluNH<sub>2</sub> with 4-(4-pyridyl)-*N*-2,4-dinitrophenylpyridinium chloride (Salt-3) caused the elimination of 2,4-dinitroaniline and resulted in a 77% yield of PFluPyPy (Scheme 3a). In order to obtain PPs that contained the viologen unit (Unit A) and the pyridylpyridinium unit (Unit B) in various molar ratios, *N*-ethylation of the 4-pyridyl group of PFluPyPy with ethyl iodide was carried out.

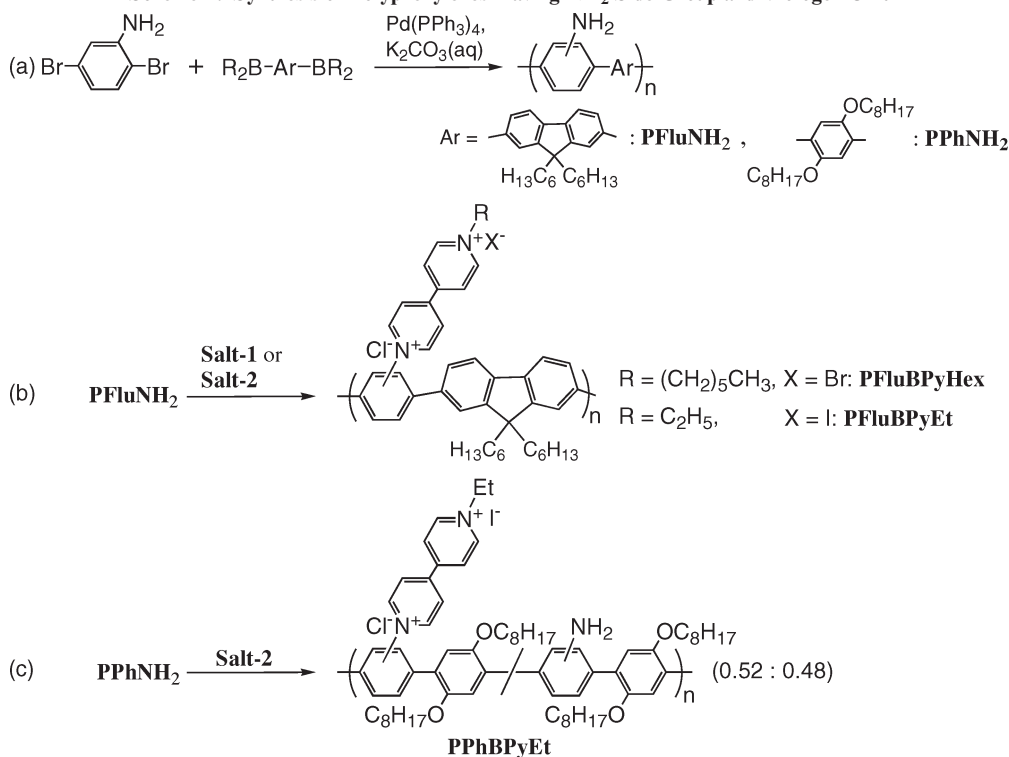
The *N*-ethylation reactions for 48 and 96 h yielded PFluPyPyEt-a and PFluPyPyEt-b which consisted of Unit A and Unit B in 0.19:0.81 and 0.72:0.28 molar ratios, respectively; these contents were determined from the <sup>1</sup>H NMR spectra.

In order to obtain information about the structures of the polymers and the structure–property relationship, several model compounds were synthesized, as shown in Scheme 4. The Suzuki coupling reaction of 9,9-dihexylfluorene-2,7-diboronic acid bis(1,3-propanediol) ester or 2,6-dioctyloxybenzene-1,4-diboronic acid with 2-bromoaniline and/or 3-bromoaniline yielded three types of model compounds with two NH<sub>2</sub> groups each. The synthesis results are summarized in Table 2. The low yield of Model-1c was ascribed to the formation of Model-1a and Model-1b when 9,9-dihexylfluorene-2,7-diboronic acid reacted with a mixture of 2-bromoaniline and 3-bromoaniline.

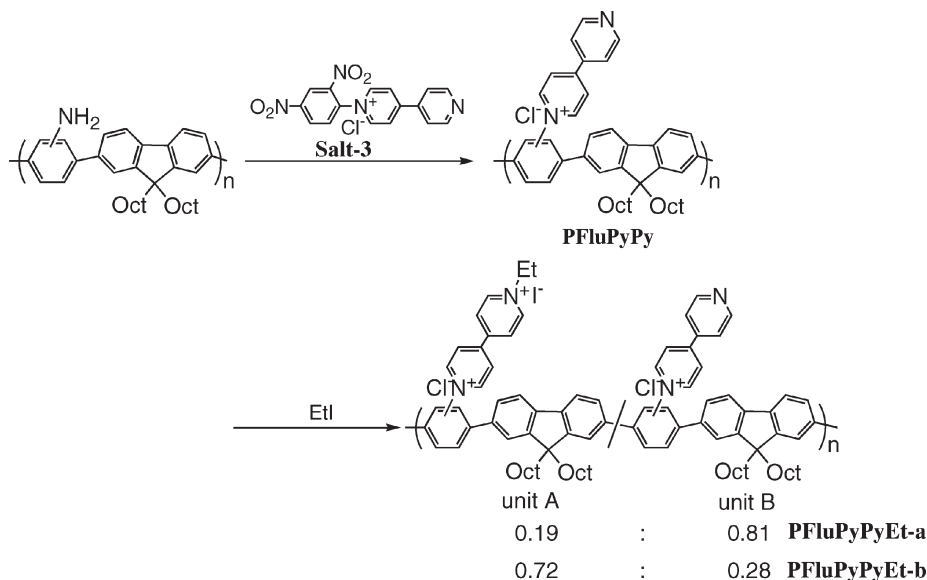
The reaction of Model-1a with Salt-2 resulted in a 41% yield of Model-3 (Scheme 5). The low yield of Model-3 was because its solubility, which is similar to that of Salt-2, made it difficult to separate the two compounds.

**<sup>1</sup>H NMR Spectra.** Figure 1 shows the <sup>1</sup>H NMR spectra of PFluNH<sub>2</sub> and PFluBPyEt. The presence of the three peaks assignable to the amine protons at  $\delta$  5.16, 5.13, and 4.92 suggests that PFluNH<sub>2</sub> has the three types of coupling units, as depicted in Figure 2. These peaks can be assigned to the NH<sub>2</sub> protons in the tail-to-tail (TT), head-to-tail (HT), and head-to-head (HH) units, respectively. This assignment is related to the chemical shifts of the NH<sub>2</sub> groups in Model-1a ( $\delta$  = 4.74), Model-1b ( $\delta$  = 5.16), and Model-1c ( $\delta$  = 5.11). The molar ratio of the TT, HT, and HH units in PFluNH<sub>2</sub> was determined to be 0.17:0.06:0.77 from the peak integrals of the NH<sub>2</sub> protons.

The signals due to aliphatic and aromatic protons of PFluNH<sub>2</sub> were observed in the ranges of  $\delta$  0.72–2.08 and  $\delta$  7.47–7.91, respectively. The observed areas of the signals due to amine, aliphatic, and aromatic protons were in good agreement with the structure of PFluNH<sub>2</sub> shown in Scheme 2a. The peak due to the NH<sub>2</sub> protons of PPhNH<sub>2</sub> was duplicated with that due to the OCH<sub>2</sub> protons, which prevented determination of the molar ratio of the TT, HT, and HH units in PPhNH<sub>2</sub>. However, the peak integrals

Scheme 2. Synthesis of Polyphenylenes Having NH<sub>2</sub> Side Group and Viologen Unit

Scheme 3. Synthesis of PPs Having Various Molar Contents of the Viologen Unit



of PPhNH<sub>2</sub> support the proposed structure shown in Scheme 2a. Data from the elemental analysis also agreed with the structures of PFluNH<sub>2</sub> and PPhNH<sub>2</sub> with hydration water; the presence of the hydrophilic NH<sub>2</sub> groups in the polymers appeared to be the reason for the hydration.

The disappearance of the peaks due to the NH<sub>2</sub> protons in the <sup>1</sup>H NMR spectrum of PFluBPyHex (Figure 1b) suggests that the reaction of PFluNH<sub>2</sub> with Salt-1 proceeded completely. The peak integral ratio of the aliphatic and aromatic protons also supports this assumption. However, PPhBPyEt showed peaks due to the pyridinium ring protons of the viologen at  $\delta$  9.47 and  $\delta$  8.93 and benzene rings in the polymer backbone in the range of  $\delta$  6.76–8.26 in a 4.08:5 ratio, respectively. This suggests that the degree of the

substitution of the NH<sub>2</sub> group with the viologen moiety was 0.52, as mentioned above. The chemical shifts in the peaks due to the pyridinium and benzene rings of PFluBPyEt were essentially the same as those of PFluBPyHex.

The degree of N-ethylation in PFluPyPyEt-a, PFluPyPyEt-b, and PFluPyPyEt-c was determined by the peak integral ratio of the pyridinium ring protons and the CH<sub>2</sub> in the N-Et group.

**IR Spectra.** As shown in Figure 3, the IR spectra of PFluNH<sub>2</sub> and PPhNH<sub>2</sub> show two distinct peaks due to  $\nu(\text{N-H})$  at 3474, 3381, 3448, and 3368 cm<sup>-1</sup>, respectively. Peaks assignable to  $\delta(\text{N-H})$  of PFluNH<sub>2</sub> and PPhNH<sub>2</sub> were observed at 1612 and 1616 cm<sup>-1</sup>, respectively. Because of the introduction of the viologen, the absorptions due to the NH<sub>2</sub> group disappeared and a new strong absorption due to

$\nu(\text{C}=\text{N})$  in the viologen unit appeared at  $1632\text{ cm}^{-1}$  in the IR spectra of PFluBPyHex and PPhBPyEt.

**Molecular Weights and Viscosities.** PFluNH<sub>2</sub> and PPhNH<sub>2</sub> were completely soluble in less-polar organic solvents such as toluene and chloroform. Furthermore, PFluNH<sub>2</sub> and PPhNH<sub>2</sub> were partly soluble in polar organic solvents such as DMF and NMP. In contrast to PFluNH<sub>2</sub> and PPhNH<sub>2</sub>, PFluBPyHex, PFluBPyEt, PPhBPyEt, PFluPyPy, PFluPyPyEt-a, PFluPyPyEt-b, and PFluPyPyEt-c were soluble in DMF and NMP but insoluble in toluene and chloroform. The lengths of the *N*-alkyl groups in PFluBPyHex and PFluBPyEt did not affect the solubilities of the polymers. GPC measurements suggested that the  $M_n$  and  $M_w$  values of PFluNH<sub>2</sub> were 20 930 and 36 090, respectively, while those of PPhNH<sub>2</sub> were 4470 and 7980,

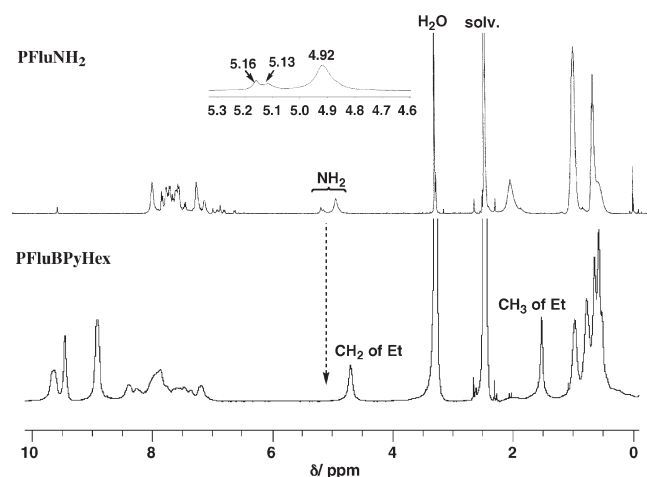


Figure 1. <sup>1</sup>H NMR spectra of PFluNH<sub>2</sub> and PFluBPyEt in DMSO-*d*<sub>6</sub>.

respectively. The molecular weights of PFluNH<sub>2</sub> and PPhNH<sub>2</sub> calculated from the elemental analysis were approximately 22 100 and 5480, respectively. It is known that the use of polystyrene standards leads to a significant overestimation of the measured molecular mass values.

DMSO solutions of PFluNH<sub>2</sub> and PPhNH<sub>2</sub> afforded intrinsic viscosities of 0.27 and 0.10 dL g<sup>-1</sup>, respectively. The  $\eta_{sp}/c$  values of PFluBPyHex, PFluBPyEt, and PPhBPyEt in DMSO increased when their concentration (*c*) was reduced, suggesting that the polymers behaved as polymeric electrolytes in the dilute solutions.<sup>20</sup> The  $\eta_{sp}/c$  values of PFluBPyHex, PFluBPyEt, and PPhBPyEt in DMSO at 30 °C were significantly larger than those of the corresponding starting polymers PFluNH<sub>2</sub> and PPhNH<sub>2</sub>. This is apparently due to the expanded structures of PFluBPyHex, PFluBPyEt, and PPhBPyEt. These structures were induced by the static repulsion between the dicationic viologen side groups in the dilute solutions. This assumption is supported by the results showing that the  $\eta_{sp}/c$  value of PFluBPyEt is higher than that of PFluPyPyEt-b.

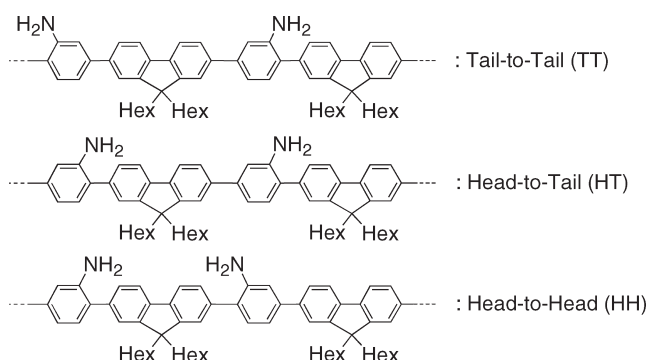
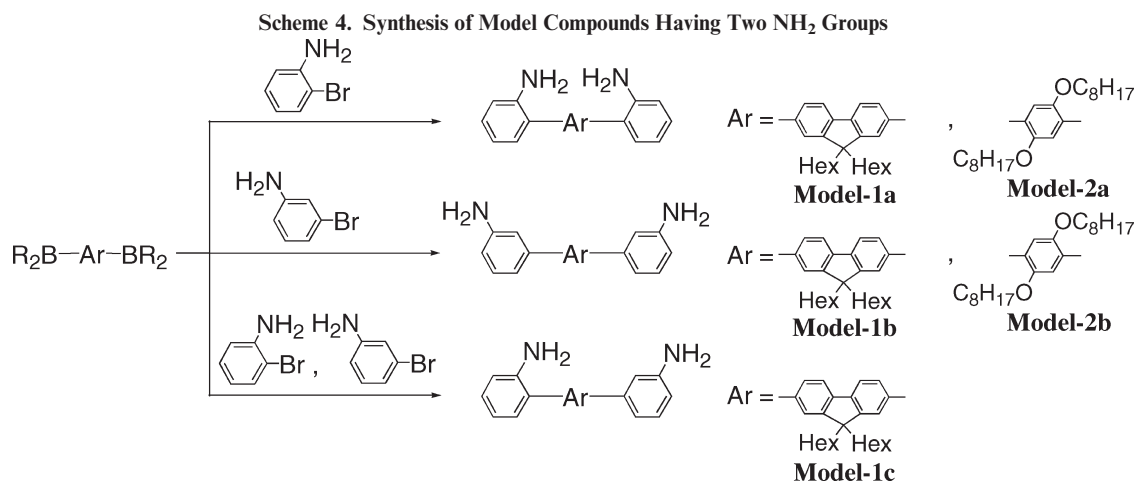
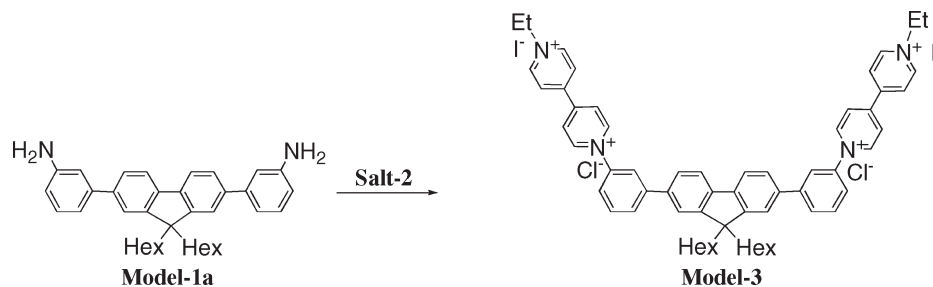
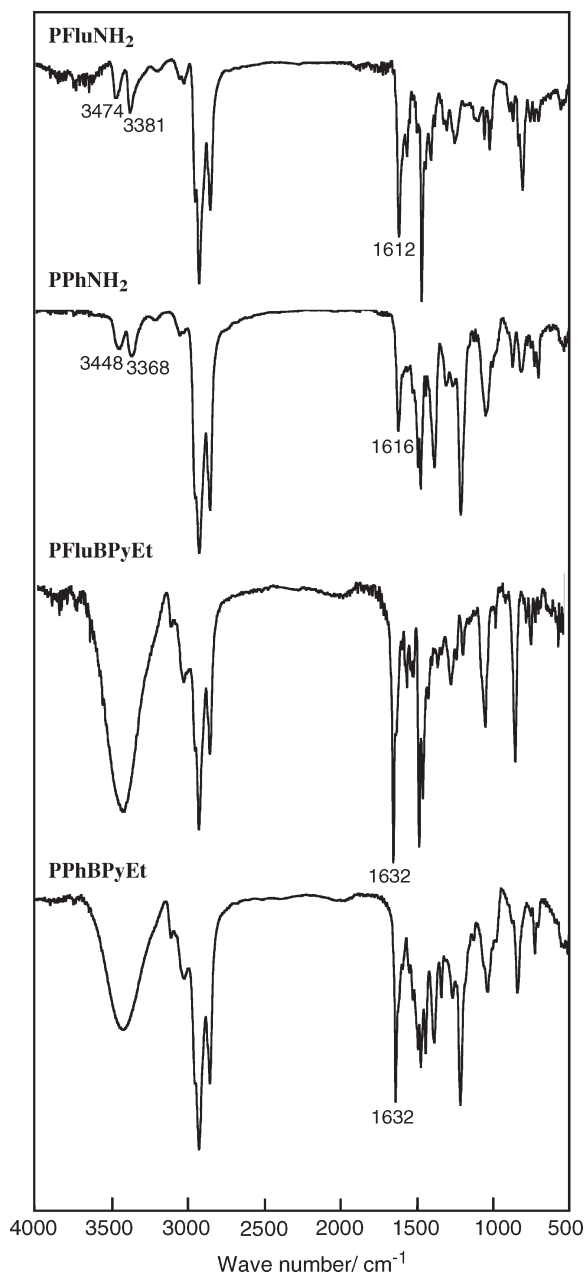


Figure 2. Structurally nonequivalent diads in PFluNH<sub>2</sub>.



**Scheme 5. Synthesis of Model Compound Having Viologen Moieties**





**Figure 3.** IR spectra of PFluNH<sub>2</sub>, PPhNH<sub>2</sub>, PFluBPyEt, and PPhBPyEt.

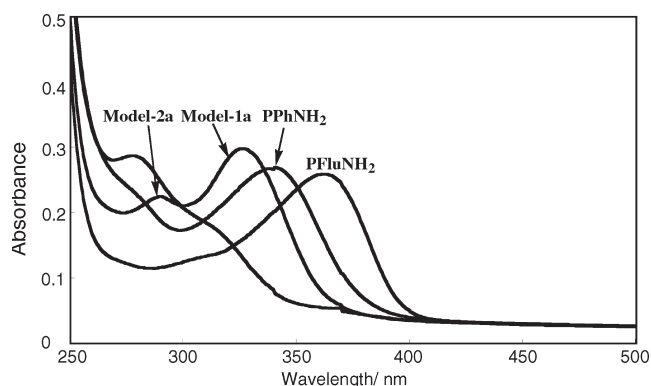
**UV–vis Absorption.** Optical data relating to the polymers and the model compounds are summarized in Tables 1 and 2, respectively. Figure 4 shows the UV–vis spectra of PFluNH<sub>2</sub>, PPhNH<sub>2</sub>, Model-1a, and Model-2a in CHCl<sub>3</sub>. PFluNH<sub>2</sub> and PPhNH<sub>2</sub> each showed an absorption maximum ( $\lambda_{\text{max}}$ ) at longer wavelengths than those of the corresponding model compounds due to the expansion of the  $\pi$ -conjugation system along the polymer chain. The observation of the  $\lambda_{\text{max}}$  of PPhNH<sub>2</sub> at a shorter wavelength than that of PFluNH<sub>2</sub> was due to the steric repulsion between the NH<sub>2</sub> and OC<sub>8</sub>H<sub>17</sub> side groups, which brought about a twisting of the polymer backbone. Model compounds having inner the NH<sub>2</sub> groups Model-1a and Model-2a each showed a  $\lambda_{\text{max}}$  at shorter wavelengths than those having the outer NH<sub>2</sub> groups Model-1b and Model-2b due to the steric hindrance of the inner NH<sub>2</sub> groups.

Figure 5 shows the UV–vis spectra of DMSO solutions of PFluBPyEt, PFluPyPyEt-a, PFluPyPyEt-b, and Model-3

**Table 2.** Synthesis Results and Optical Properties of Model Compounds

	yield (%)	absorption/nm	$\lambda_{\text{em}}$ /nm <sup>c</sup>
Model-1a	81	329 <sup>a</sup>	455 (0.39)
Model-1b	73	332 <sup>a</sup>	470 (0.32)
Model-1c	36	326 <sup>a</sup>	457 (0.35)
Model-2a	62	307 <sup>a</sup>	403 (0.04)
Model-2b	53	319 <sup>a</sup>	391 (0.05)
Model-3	41	366 <sup>b</sup>	

<sup>a</sup> In CHCl<sub>3</sub>. <sup>b</sup> In DMSO. <sup>c</sup> Photoluminescence (PL) peak in CHCl<sub>3</sub>. Quantum yields of PL were shown in parentheses.



**Figure 4.** UV–vis spectra of PFluNH<sub>2</sub>, PPhNH<sub>2</sub>, Model-1a, and Model-2a in CHCl<sub>3</sub>.

under nitrogen and in air. The absorption peak due to the  $\pi$ – $\pi^*$  transitions of PFluBPyEt was observed at 364 nm; this wavelength was longer than that of Model-3. The UV–vis spectrum of PFluBPyEt under a nitrogen atmosphere showed a shoulder peak at 400 nm and four peaks in the range of 570–680 nm; these peaks were assignable to the viologen radical cation that was formed by the electron transfer from the polymer backbone to the viologen. These peak positions are consistent with earlier reports of the peaks of the viologen radical cation bonded to polythiophene.<sup>10b</sup> The blue DMSO solution of PFluBPyEt under the nitrogen atmosphere gradually changed to a colorless solution when it stood in air. This color change was comparable to the result that the absorptions due to the viologen radical cation were disappeared in air. This indicated that the viologen radical of PFluBPyEt was unstable in air. It is known that the viologen radical cation reacts with oxygen and reverts back to the viologen moiety.<sup>21</sup> In fact, bubbling of oxygen gas into the blue solution of PFluBPyEt immediately resulted in a change to a colorless solution. Absorption due to the pyridine radical was not observed in the UV–vis spectrum of PFluPyPy. The above UV–vis results confirmed that the electron transfer from the polymer backbone to the electron-accepting viologen was responsible for the formation of the viologen radical cation. PFluPyPyEt-a and PFluPyPyEt-b showed absorptions due to the radical cation of viologen at essentially the same positions as in PFluBPyEt. However, the peaks due to the viologen radical cation of PFluPyPyEt-a and PFluPyPyEt-b were much smaller than those of PFluBPyEt. These results suggested that the formation of the viologen radical cation strongly depended on the content of the viologen moiety in the polymers.

The wavelengths at which absorptions due to the  $\pi$ – $\pi^*$  transitions of PFluBPyEt were observed were longer than those of Model-3. The absorptions due to the viologen radical cation of Model-3 were smaller than those of PFluBPyEt, as shown in Figure 5. This result indicates that the electron transfer to the viologen moiety occurred easily in the



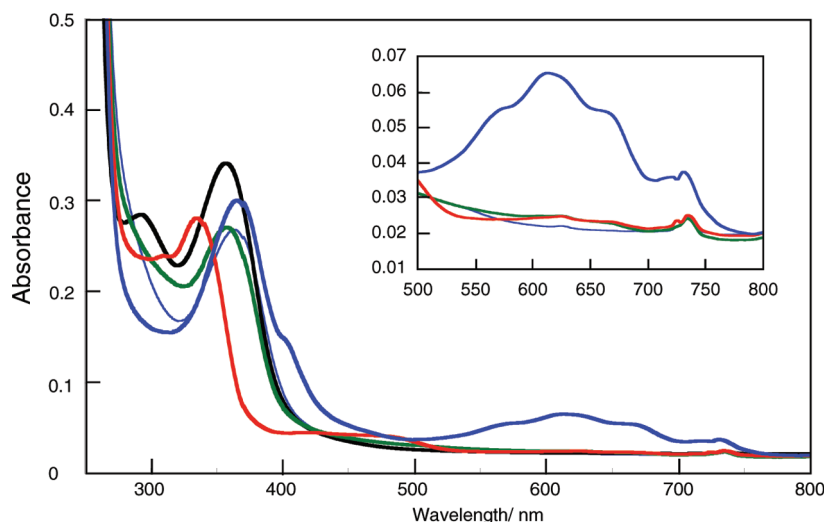


**Figure 5.** UV-vis spectra of the DMSO solutions of PFluBPyEt (blue curve), PFluPyPyEt-a (green curve), PFluPyPyEt-b (black curve), and Model-4 (red curve) under nitrogen and the DMSO solution of PFluBPyEt (blue thin curve) in air.

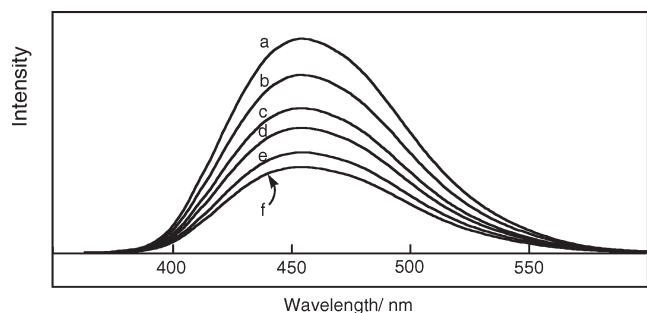


**Figure 6.** PL spectra of DMSO solutions of PPhNH<sub>2</sub> ( $1.0 \times 10^{-5}$  M) in the presence of a series of concentrations of EV<sup>2+</sup>. [EV<sup>2+</sup>] = 0 (a),  $1.7 \times 10^{-4}$  (b),  $3.4 \times 10^{-4}$  (c),  $5.1 \times 10^{-4}$  (d),  $6.8 \times 10^{-4}$  (e), and  $8.5 \times 10^{-4}$  M (f).

case of PFluBPyEt because it had a longer expanded  $\pi$ -conjugation system than Model-3.

**Photoluminescence.** PFluNH<sub>2</sub>, PPhNH<sub>2</sub>, and the model compounds (except for Model-3) were photoluminescent in solution when irradiated with UV light. The photoluminescence (PL) peak of the polymers and model compounds appeared at an onset position of the their absorption bands, as usually observed with photoluminescent polyphenylenes.<sup>16</sup> The quantum yields of the PL of PFluNH<sub>2</sub> and PPhNH<sub>2</sub> in chloroform were 0.10 and 0.03, respectively. In contrast to PFluNH<sub>2</sub>, PPhNH<sub>2</sub>, and Model-1a, PFluBPyEt, PPhBPyEt, and Model-3 showed no PL in solution. This result is consistent with the fact that viologens brought about a quenching effect on photoluminescent compounds.<sup>22</sup> In order to confirm that the quenching of PL in PFluBPyEt and PPhBPyEt was because these polymers contained the viologen moiety, PL measurements of PFluNH<sub>2</sub> and PPhNH<sub>2</sub> in the presence of 1,1'-ethyl-4,4'-bipyridyl (ethyl viologen; EV<sup>2+</sup>) were conducted.

Figure 6 shows the PL spectra of PPhNH<sub>2</sub> and PPhNH<sub>2</sub> in the presence of a series of concentrations of EV<sup>2+</sup>. The PL intensities decreased with an increase in the amount of EV<sup>2+</sup>. A quantitative measurement of the PL quenching can be achieved by determining the Stern–Volmer constant,  $K_{SV}$ :

$$I_0/I = 1 + K_{SV}[\text{quencher}]$$

where  $I_0$  is the intensity of the PL in the absence of the quencher and  $I$  is the intensity of the PL in the presence of the

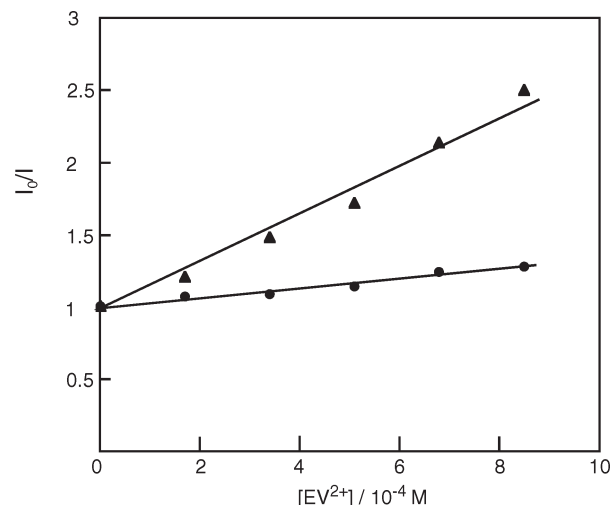


**Figure 7.** Stern–Volmer plots for PL quenching by EV<sup>2+</sup> for PFluNH<sub>2</sub> and PPhNH<sub>2</sub>.

quencher. The equation reveals that  $I_0/I$  increases in direct proportion to the concentration of the quenching moiety, and the constant  $K_{SV}$  defines the efficiency of quenching. Figure 7 shows Stern–Volmer plots for PL quenching by EV<sup>2+</sup> for PFluNH<sub>2</sub> and PPhNH<sub>2</sub>. The  $K_{SV}$  values of PFluNH<sub>2</sub> and PPhNH<sub>2</sub> were  $3.3 \times 10^2$  and  $1.8 \times 10^3$  M<sup>−1</sup>, respectively. These values were considerably lower than those of water-soluble anionic  $\pi$ -conjugated polymers reported earlier; those polymers had  $K_{SV}$  values as high as  $10^5$ – $10^8$  M<sup>−1</sup>.<sup>22</sup> The high efficiency of the PL quenching can be attributed to the easy formation of an associate complex between water-soluble anionic polymers and cationic viologens in water. The low efficiency of the quenching of PFluNH<sub>2</sub> and PPhNH<sub>2</sub> by the viologen appeared to be due to the fact that the neutral structures of the polymers made it difficult for the polymers to form an associate complex with the viologen. The  $K_{SV}$  value of PFluNH<sub>2</sub> was lower than that of PPhNH<sub>2</sub> because the hexyl groups at the 9,9-positions of the fluorene unit that might be a steric hindrance to form an associate complex with EV<sup>2+</sup>. It is known that the alkyl groups at the 9,9-positions of the fluorene unit were located perpendicular to the plane of the fluorene group.<sup>23</sup>

**ESR.** In order to confirm the presence of the viologen radical in PFluBPyEt, ESR measurements were conducted.

Figure 8 shows the ESR spectrum of PFluBPyEt at 293 K under nitrogen. The ESR spectrum of PFluBPyEt gave a symmetric signal with a peak-to-peak line width of  $\Delta H_{pp} = 0.30$  G, a spin density of  $2.0 \times 10^{17}$  spins/g, and a  $g$ -value of  $g = 2.0067$ . It has been reported that Na-doped poly(*p*-phenylene) (PPP) shows a symmetrical ESR signal with a peak-to-peak line width of  $\Delta H_{pp} = 0.18$  G, a spin density of  $1.6 \times 10^{19}$  spins/g, and a  $g$ -value of  $g = 2.0027$ .<sup>24</sup> The bulky side chain group bonded to the  $\pi$ -conjugated polymer backbone often results in the bond twisting along the polymer backbone and reduces the extent of polaron delocalization along the polymer backbone.<sup>9</sup> For PFluBPyEt, the bulky viologen moiety may induce an additional twisting of the ring along the polymer backbone due to the increased steric hindrance. This effect is apparently reflected by the fact that PFluBPyEt has a higher  $\Delta H_{pp}$  than that of Na-doped PPP in the ESR spectra

**Electrochemical and Electric Properties.** The cyclic voltammetry measurement suggests that a cast film of PFluB-

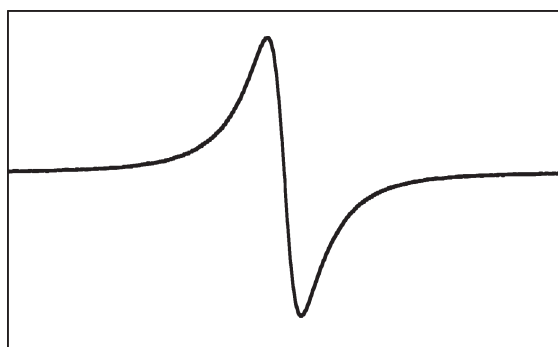


Figure 8. ESR spectrum of PFluBPyEt at 293 K.

PyEt on a Pt plate undergoes two-step electrochemical reduction in the viologen moiety and electrochemical oxidation of the polymer backbone in an acetonitrile solution of 0.10 M  $[\text{NEt}_4]\text{BF}_4$ . The peak potentials are summarized in Table 2. As depicted in Figure 9a, the cyclic voltammogram of PFluBPyEt shows the first peak cathode potential  $E_{pc}(1)$  and the second peak cathode potential  $E_{pc}(2)$  at  $-0.78$  and  $-1.23$  V vs  $\text{Ag}^+/\text{Ag}$ , respectively; these were coupled with anode potentials  $E_{pa}(1)$  and  $E_{pa}(2)$  at  $-0.54$  and  $-1.02$  V vs  $\text{Ag}^+/\text{Ag}$ , respectively. PFluBPyEt showed an anodic peak at 1.53 V due to the electrochemical oxidation of the polymer backbone. However, the corresponding reduction (p-dedoping) peak did not appear in the cyclic voltammograms; this is likely because of the formation of a stable adduct between the dicationic viologen moieties of the polymers and  $\text{BF}_4^-$ , which prevented electrochemical reduction (p-dedoping). It has been reported that  $\pi$ -conjugated polymers having a viologen side group show an irreversible electrochemical oxidation.<sup>4b</sup> The magnitude of the anodic peak was in the range of 0–2.0 V, and this is likely due to the electrochemical oxidation of the polymer backbone. This is a much smaller value than was obtained when the applied potential was swept to a value that was enough to reduce the viologen moieties to a monovalent state ( $\text{V}^{\bullet+}$ ), as shown in Figure 9b.

This result can be explained by the viologen-mediated electron transfer reaction; the monovalent viologen takes part in dedoping the polymer backbone (Figure 10). The electron migration between the polymer backbone and the viologen moiety appears to be because the structures of the polymers contained the viologen moieties at the side chains of the  $\pi$ -conjugated polymer backbone.

The brown film of PFluBPyEt changed to dark green after the electrochemical reduction and returned to brown after crossing the  $E_{pa}(2)$  peak. The brown films changed to

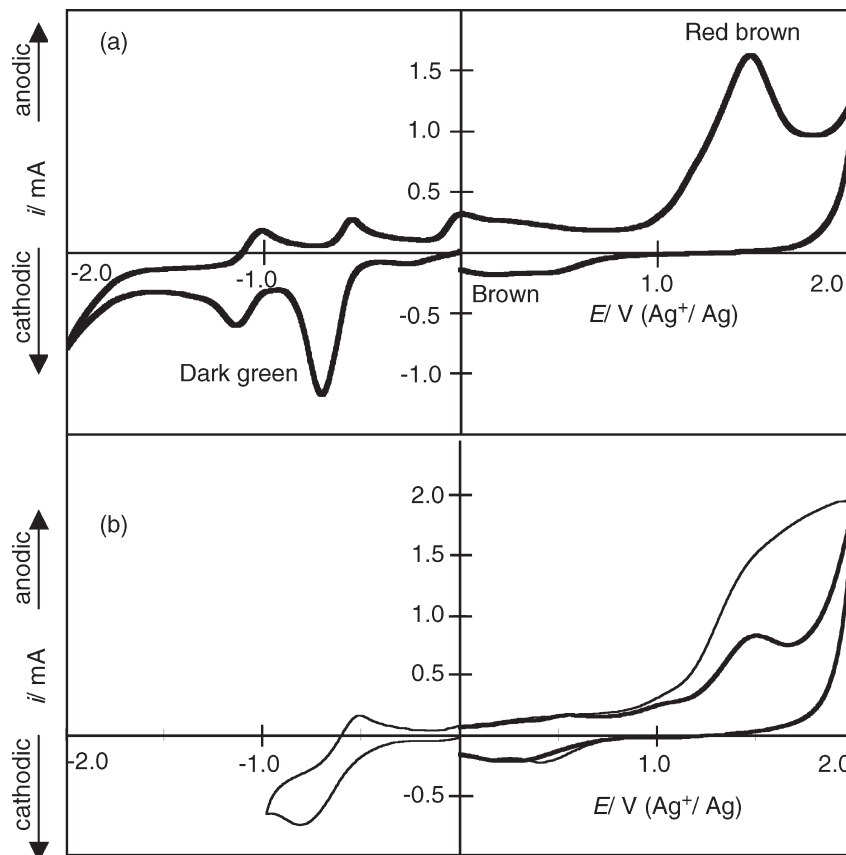
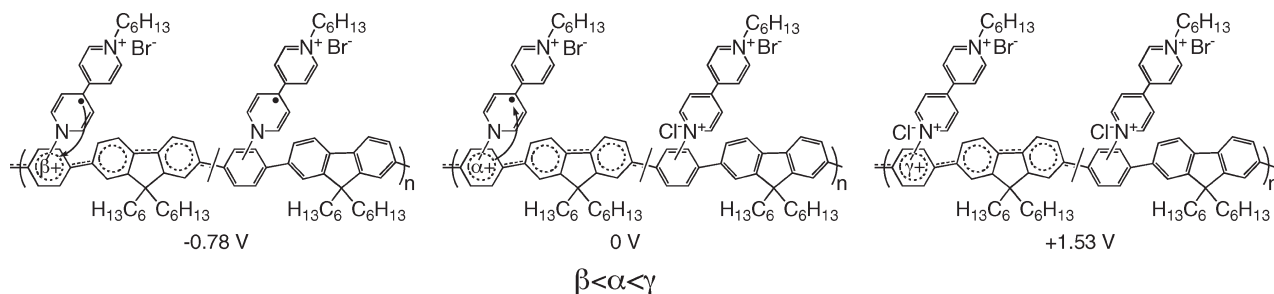
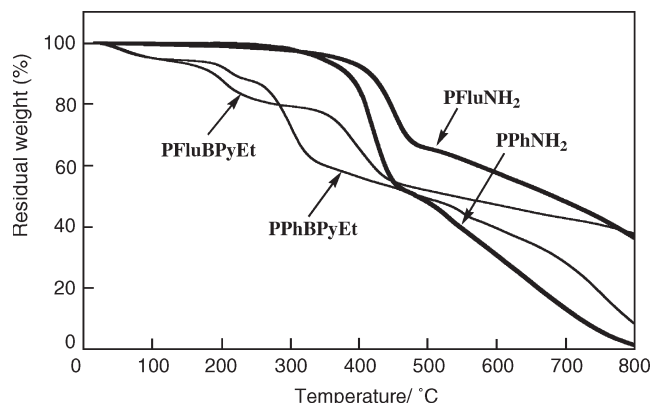


Figure 9. Cyclic voltammograms of a cast film of PFluBPyEt on a Pt plate in a DMSO solution of  $[\text{Et}_4\text{N}]\text{BF}_4$  (0.10 M). The scan rate was  $50 \text{ mV s}^{-1}$ .



**Figure 10.** Schematic view of viologen-mediated electron transfer mechanism.



**Figure 11.** TGA curves of PFluNH<sub>2</sub>, PPhNH<sub>2</sub>, PFluBPyEt, and PPhBPyEt with a heating rate of 10 °C/min under nitrogen.

red-brown after electrochemical oxidation. Nearly the same electrochromism was observed in PFluBPyHex, PPhBPyEt, PFluPyPyEt-a, and PFluPyPyEt-b.

The electric conductivities ( $\sigma$ ) of the pellets molded from PFluBPyEt and PPhBPyEt were  $6.4 \times 10^{-6}$  and  $1.1 \times 10^{-6}$  S cm<sup>-1</sup>, respectively. These  $\sigma$  values were higher than those of PFluNH<sub>2</sub> and PPhNH<sub>2</sub> ( $\sigma < 10^{-8}$  S cm<sup>-1</sup>, respectively), supporting the assumption that self-doping occurs in PFluBPyEt and PPhBPyEt. The fact that PPhBPyEt had a lower conductivity than PFluBPyEt was due to the twisting of the polymer backbone of PPhBPyEt, which was brought about by the steric repulsion between the viologen and OC<sub>8</sub>H<sub>17</sub> groups. The electric conductivities of PFluBPyEt and PPhBPyEt were 1 order smaller than that of the iodine-doped poly(*p*-phenylene) ( $\sigma = 7 \times 10^{-5}$  S cm<sup>-1</sup>).<sup>25</sup> The origin of the lower conductivity appears to be due to the ring twisting along the polymer backbone, which was induced by the steric hindrance of the bulky viologen moiety. This inference is consistent with the UV-vis results described above.

**Thermal Properties.** Figure 11 shows the TGA curves of PFluNH<sub>2</sub>, PPhNH<sub>2</sub>, PFluBPyEt, and PPhBPyEt. PFluNH<sub>2</sub> and PPhNH<sub>2</sub> showed good thermal stability up to 300 °C, while PFluBPyEt and PPhBPyEt started thermal weight loss at lower temperatures. The 5% weight loss temperatures of PFluNH<sub>2</sub> and PPhNH<sub>2</sub> were 344 and 328 °C, respectively; the higher thermal stabilities of PFluNH<sub>2</sub> than PPhNH<sub>2</sub> appear to correspond with their higher molecular weights. The weight loss of PFluBPyEt and PPhBPyEt in the range of 80–180 °C corresponds to the thermal loss of hydrated water in PFluBPyEt and PPhBPyEt. The content of hydrated water in PFluBPyEt and PPhBPyEt was confirmed by the IR spectra. PFluBPyEt and PPhBPyEt exhibited a two-stage thermal decomposition process, with the second decomposition occurring at around 330 °C for PFluBPyEt and 260 °C for PPhBPyEt. In the second thermal decomposition stage, PFluBPyEt and PPhBPyEt showed a weight loss of 22 and

28 wt %, respectively. These values are largely consistent with the content of the alkyl groups in the polymers, suggesting that the second thermal decomposition was attributed to loss of the alkyl of the polymers.

## Conclusions

PPs that contain viologen side groups (PFluBPyHex, PFluBPyEt, and PPhBPyEt) were obtained by the reaction using PPs having a NH<sub>2</sub> side group as starting materials. The UV-vis and ESR spectra of the polymers suggest the formation of the viologen radical cation, which was generated by the electron transfer from the polymer backbone to the viologen moiety. PFluBPyHex, PFluBPyEt, and PPhBPyEt were electrochemically active in film, and the electrochemical reaction was accompanied by electrochromism. The electric conductivities of the molded PFluBPyEt and PPhBPyEt pellets were 3 orders of magnitude higher than those of PFluNH<sub>2</sub> and PPhNH<sub>2</sub> because of the self-doping nature of PFluBPyEt and PPhBPyEt. From the results obtained in this study, it can be concluded that new conducting materials can be developed on the basis of the ability of the viologen to be a p-dopant for  $\pi$ -conjugated polymers.

## Experimental Section

**General.** Solvents were dried, distilled, and stored under nitrogen. 2,6-Dioctyloxybenzene-1,4-diboronic acid and *N*-(2,6-dinitrophenyl)-4-pyridylpyridinium chloride were prepared according to the literature.<sup>18,26</sup> Other reagents were purchased and used without further purification. Reactions were carried out with standard Schlenk techniques under nitrogen.

IR and NMR spectra were recorded on a JASCO FT/IR-660 PLUS spectrophotometer and a JEOL AL-400 spectrometer, respectively. Elemental analysis was carried out on a Yanagimoto MT-5 CHN coder. UV-vis and PL spectra were obtained by a JASCO V-560 spectrometer and a JASCO FP-6200, respectively. Quantum yields were calculated by using a diluted ethanol solution of 7-(dimethylamino)-4-methylcoumarin as the standard. Molecular weights were obtained by SEC with a Jasco 830-RI refractometer with polystyrene gel columns (K-803 and K-804) using chloroform as an eluent. Cyclic voltammetry was performed in a DMSO solution containing 0.10 M [Et<sub>4</sub>N]BF<sub>4</sub> with a BAS 100B. Electric conductivity measurements were carried out with a HORIBA COND METER ES-51 using a four-probe method. TGA curves were obtained by a Rigaku Thermo plus TG8120.

**Synthesis of Salt-1.** After an EtOH solution (5 mL) of *N*-hexyl-4-pyridylpyridinium bromide (0.94 g, 3.0 mmol) and 1-chloro-2,4-dinitrobenzene (0.73 g, 3.6 mmol) was refluxed for 48 h, the solvent removed by evaporation. The resulting solid was washed with CHCl<sub>3</sub> at 50 °C, filtrated at the temperature, and dried under vacuum to give Salt-1 as a red powder (1.5 g, 88%). <sup>1</sup>H NMR (400 MHz, DMSO-*d*<sub>6</sub>):  $\delta$  9.76 (s, 2H), 9.51 (s, 2H), 9.15 (m, 3H), 8.98–9.04 (m, 3H), 8.50 (d, *J* = 8.4 Hz, 1H), 4.74 (s, 2H), 2.00 (s, 2H), 1.29–1.32 (m, 6H), 0.87 (t, *J* = 6.8 Hz, 3H). <sup>13</sup>C{<sup>1</sup>H} NMR (100 MHz, DMSO-*d*<sub>6</sub>):  $\delta$  151.3, 149.3, 147.9, 147.2, 146.0, 143.0, 138.3, 132.1, 130.3, 127.0,



126.5, 121.5, 61.0, 30.8, 30.6, 25.1, 21.9, 13.9. Calcd for  $C_{18}H_{16}N_4ClO_4 \cdot 0.9H_2O$ : C, 40.72; H, 3.38; N, 10.55. Found: C, 40.71; H, 3.26; N, 9.96.

Salt-2 was synthesized analogously.

**Data of Salt-2.**  $^1H$  NMR (400 MHz, DMSO- $d_6$ ):  $\delta$  9.73 (d,  $J$  = 6.8 Hz, 2H), 9.50 (d,  $J$  = 6.8 Hz, 2H), 9.16 (d,  $J$  = 2.4 Hz, 1H), 9.11 (d,  $J$  = 6.8 Hz, 2H), 9.04 (dd,  $J$  = 2.8 and 8.8 Hz, 1H), 8.95 (d,  $J$  = 6.8 Hz, 2H), 8.47 (d,  $J$  = 8.4 Hz, 1H), 4.77 (q,  $J$  = 7.6 Hz, 2H), 1.63 (t,  $J$  = 7.6 Hz, 3H).  $^{13}C\{^1H\}$  NMR (100 MHz, DMSO- $d_6$ ):  $\delta$  151.3, 149.3, 147.9, 147.2, 145.8, 143.0, 138.3, 132.0, 130.3, 126.9, 126.4, 121.5, 56.7, 16.3. Calcd for  $C_{22}H_{24}BrClN_4O_4 \cdot H_2O$ : C, 48.77; H, 4.84; N, 10.34. Found: C, 49.05; H, 5.00; N, 10.34.

**Synthesis of PFluNH<sub>2</sub>.** 2,5-Dibromoaniline (0.50 g, 2.0 mmol) and 9,9-dihexylfluorene-2,7-diboronic acid bis(1,3-propanediol) ester (1.0 g, 2.0 mmol) were dissolved in 20 mL of dry toluene under N<sub>2</sub>. To the solution were added K<sub>2</sub>CO<sub>3</sub>(aq) (2.0 M, 10 mL; N<sub>2</sub> bubbled before use), Pd(PPh<sub>3</sub>)<sub>4</sub> (0.23 g, 0.20 mmol), and several drops of Aliquat336 as a phase transfer catalyst. After the mixture was stirred at 80 °C for 72 h, the solvent was removed under vacuum. The resulting solid was extracted with chloroform and reprecipitated in methanol. PFluNH<sub>2</sub> was collected by filtration, dried under vacuum, and obtained as a light brown powder (0.83 g, 98%).  $^1H$  NMR (400 MHz, DMSO- $d_6$ ):  $\delta$  7.91–7.47 (9H), 5.16 (s, 0.28 H), 5.12 (s, 0.14H), 4.92 (s, 1.58H), 2.08 (s, 4H), 1.04 (s, 12H), 0.72 (m, 10H).  $^{13}C\{^1H\}$  NMR (100 MHz, CDCl<sub>3</sub>):  $\delta$  151.6, 144.3, 143.9, 142.2, 140.2, 139.3, 132.8, 131.8, 131.0, 127.7, 125.9, 123.7, 121.4, 120.0, 118.5, 117.8, 114.3, 108.3, 55.3, 40.4, 31.5, 29.7, 23.9, 22.6, 14.0. Calcd for Br(C<sub>31</sub>H<sub>37</sub>N)<sub>58</sub>B(OH)<sub>2</sub>: C, 85.96; H, 9.79; N, 3.68; Br, 0.36. Found: C, 85.53; H, 6.40; N, 3.49; Br, 0.36.

PPhNH<sub>2</sub> was synthesized analogously. Spectroscopic and analytical data of the polymer are shown below.

**Data of PPhNH<sub>2</sub>.**  $^1H$  NMR (400 MHz, CDCl<sub>3</sub>):  $\delta$  7.00–7.43 (5H), 3.96 (s, 6H), 1.69–1.75 (4H), 1.25–1.34 (20H), 0.87 (6H).  $^{13}C\{^1H\}$  NMR (100 MHz, CDCl<sub>3</sub>):  $\delta$  150.7, 150.6, 150.4, 144.2, 138.5, 138.5, 132.2, 130.9, 129.2, 128.8, 128.4, 127.9, 124.2, 120.0, 117.4, 117.2, 117.0, 116.5, 116.4, 70.3, 70.0, 69.8, 69.5, 31.8, 29.34, 29.25, 26.1, 25.9, 22.7, 14.1. Calcd for Br(C<sub>28</sub>H<sub>41</sub>NO<sub>2</sub>)<sub>33</sub>B(OH)<sub>2</sub>: C, 78.68; H, 9.67; N, 3.28; Br, 0.57. Found: C, 78.53; H, 9.47; N, 3.04; Br, 0.57.

**Synthesis of PFluBPyHex.** To a DMSO solution (5 mL) of Salt-1 (0.37 g, 0.70 mmol) was added to a CHCl<sub>3</sub> solution (10 mL) of PFluNH<sub>2</sub> (0.20 g, 0.47 mmol). After the reaction solution was stirred at 80 °C for 24 h, the solvents were removed under vacuum. The resulting solid was dissolved in DMSO (ca. 1 mL) and precipitated in water and acetone. PFluNH<sub>2</sub>Hex was collected by filtration, dried under vacuum, and obtained as a black solid (0.32 g, 89%).  $^1H$  NMR (400 MHz, DMSO- $d_6$ ):  $\delta$  9.69 (s, 2H), 9.50 (s, 2H), 8.97 (s, 4H), 7.22–8.41 (9H), 4.71 (s, 2H), 1.93 (s, 2H), 1.28 (s, 4H), 1.01 (s, 2H), 0.62–0.84 (29H). Calcd for Br(C<sub>47</sub>H<sub>56</sub>N<sub>2</sub>BrCl·2H<sub>2</sub>O)<sub>58</sub>B(OH)<sub>2</sub>: C, 69.14; H, 7.18; N, 3.44. Found: C, 69.53; H, 7.59; N, 3.91.

PFluBPyEt, PPhBPyEt, and PFluPyPy were synthesized analogously. Spectroscopic and analytical data of the polymer are shown below.

**Data of PFluBPyEt.**  $^1H$  NMR (400 MHz, DMSO- $d_6$ ):  $\delta$  9.62 (2H), 9.45 (2H), 8.92 (4H), 7.19–8.40 (9H), 4.71 (2H), 1.53 (3H), 0.53–1.09 (26H). Calcd for Br(C<sub>43</sub>H<sub>48</sub>N<sub>2</sub>ClI·2H<sub>2</sub>O)<sub>58</sub>B(OH)<sub>2</sub>: C, 65.10; H, 6.61; N, 3.53. Found: C, 65.48; H, 6.31; N, 4.00.

**Data of PPhBPyEt.**  $^1H$  NMR (400 MHz, DMSO- $d_6$ ):  $\delta$  9.47 (2.08H), 8.93 (2.08H), 6.76–8.26 (5H), 4.76 (1.04H), 3.50–4.10 (4.96H), 0.78–1.71 (31.56H). Calcd for Br{(C<sub>40</sub>H<sub>52</sub>N<sub>2</sub>·O<sub>2</sub>ClI)<sub>0.52</sub>(C<sub>28</sub>H<sub>41</sub>NO<sub>2</sub>)<sub>0.48</sub>·H<sub>2</sub>O}<sub>33</sub>B(OH)<sub>2</sub>: C, 65.13; H, 7.75; N, 2.53. Found: C, 65.46; H, 6.98; N, 2.56.

**Data of PFluPyPy.**  $^1H$  NMR (400 MHz, DMSO- $d_6$ ):  $\delta$  9.51 (2H), 8.85 (4H), 7.12–8.29 (11H), 0.58–2.10 (26H).

**Synthesis of PFluBPyEt-a.** After a MeOH solution (10 mL) of PFluPyPy (30 mg, 0.050 mmol) and ethane iodide (0.78 g, 5.0 mmol) was stirred at 55 °C for 48 h, the solvent and

unreacted ethane iodide were removed under vacuum. The resulting solid was dissolved in DMSO (ca. 1 mL) and reprecipitated in MeOH. PFluBPyEt-a was collected by filtration, dried under vacuum, and obtained as a reddish-brown solid (20 mg, 70%).  $^1H$  NMR (400 MHz, DMSO- $d_6$ ):  $\delta$  9.33–9.65 (4H), 8.72–8.93 (4H), 7.12–8.39 (9H), 4.72 (0.38H), 0.30–2.07 (26.57H). Calcd for Br{(C<sub>43</sub>H<sub>48</sub>N<sub>2</sub>ClI)<sub>0.19</sub>(C<sub>41</sub>H<sub>43</sub>N<sub>2</sub>Cl)<sub>0.81</sub>}<sub>58</sub>B(OH)<sub>2</sub>: C, 76.83; H, 7.16; N, 4.33. Found: C, 77.58; H, 7.21; N, 3.91.

PFluBPyEt-b was synthesized by stirring the solution of PFluPyPy and ethane iodide for 96 h.

**Data of PFluBPyEt-b.**  $^1H$  NMR (400 MHz, DMSO- $d_6$ ):  $\delta$  9.65 (2H), 9.44 (2H), 8.93 (4H), 7.24–8.38 (9H), 4.72 (1.44H), 0.63–2.07 (28.16H). Calcd for Br{(C<sub>43</sub>H<sub>48</sub>N<sub>2</sub>ClI)<sub>0.72</sub>(C<sub>41</sub>H<sub>43</sub>N<sub>2</sub>Cl)<sub>0.28</sub>}<sub>58</sub>B(OH)<sub>2</sub>: C, 69.87; H, 6.71; N, 3.84. Found: C, 69.58; H, 6.57; N, 3.91.

**Synthesis of Model-1a.** 2-Bromoaniline (0.69 g, 4.0 mmol) and 9,9-dihexylfluorene-2,7-diboronic acid bis(1,3-propanediol) ester (1.0 g, 2.0 mmol) were dissolved in 20 mL of dry toluene under N<sub>2</sub>. To the solution were added K<sub>2</sub>CO<sub>3</sub>(aq) (2.0 M, 10 mL; N<sub>2</sub> bubbled before use), Pd(PPh<sub>3</sub>)<sub>4</sub> (0.23 g, 0.20 mmol), and several drops of the phase transfer catalyst (Aliquat336). After the mixture was stirred at 80 °C for 72 h, the solvent was removed under vacuum. The resulting solid was extracted with chloroform and dried under vacuum to give a yellow solid, which was purified by silica gel column chromatography (eluent = CHCl<sub>3</sub>). The solvent was removed by evaporation, and a resulting solid was dried in vacuo to give Model-1a as a yellow solid (0.83 g, 81%).  $^1H$  NMR (400 MHz, CDCl<sub>3</sub>):  $\delta$  7.78 (d,  $J$  = 8.4 Hz, 2H), 7.46 (s, 2H), 7.44 (d,  $J$  = 7.6 Hz, 2H), 7.25 (d,  $J$  = 7.6 Hz, 2H), 7.22 (d,  $J$  = 7.6 Hz, 2H), 6.87 (t,  $J$  = 6.8 Hz, 2H), 3.82 (s, 4H), 1.98 (m, 2H), 2.02 (m, 4H), 1.24–1.04 (m, 10H), 0.78–0.74 (m, 8H).  $^{13}C\{^1H\}$  NMR (100 MHz, CDCl<sub>3</sub>):  $\delta$  151.5, 143.5, 139.8, 138.2, 130.5, 128.4, 128.1, 127.7, 123.7, 120.0, 118.7, 115.7, 55.3, 40.2, 31.5, 29.7, 24.0, 22.5, 14.0. Calcd for C<sub>37</sub>H<sub>44</sub>N<sub>2</sub>·0.1H<sub>2</sub>O: C, 85.70; H, 8.59; N, 5.40. Found: C, 85.68; H, 8.26; N, 5.19.

Model-1b, Model-1c, Model-2a, and Model-2b were synthesized analogously. Spectroscopic and analytical data of the polymer are shown below.

**Data of Model-1b.**  $^1H$  NMR (400 MHz, CDCl<sub>3</sub>):  $\delta$  7.74 (d,  $J$  = 8.0 Hz, 2H), 7.56 (s, 2H), 7.55 (d,  $J$  = 7.6 Hz, 2H), 7.25 (d,  $J$  = 7.6 Hz, 2H), 7.08 (d,  $J$  = 7.6 Hz, 2H), 7.00 (s, 2H), 6.71 (d,  $J$  = 7.6 Hz, 2H), 3.85 (br, 4H), 2.02 (m, 4H), 1.10–1.26 (12H), 0.77–0.88 (10H).  $^{13}C\{^1H\}$  NMR (100 MHz, CDCl<sub>3</sub>):  $\delta$  151.5, 148.7, 142.9, 140.12, 140.08, 129.7, 125.9, 121.5, 119.8, 117.7, 114.0, 113.9, 55.2, 40.5, 31.5, 29.7, 23.8, 22.6, 14.0. Calcd for C<sub>37</sub>H<sub>44</sub>N<sub>2</sub>: C, 86.00; H, 8.58; N, 5.42. Found: C, 85.82; H, 8.92; N, 5.20.

**Data of Model-1c.**  $^1H$  NMR (400 MHz, CDCl<sub>3</sub>):  $\delta$  7.77 (d,  $J$  = 8.0 Hz, 1H), 7.74 (d,  $J$  = 8.0 Hz, 1H), 7.55 (d,  $J$  = 8.0 Hz, 1H), 7.54 (s, 1H), 7.44 (s, 1H), 7.74 (d,  $J$  = 8.0 Hz, 1H), 7.28 (d,  $J$  = 7.6 Hz, 1H), 7.21 (d,  $J$  = 8.0 Hz, 1H), 7.17 (d,  $J$  = 7.6 Hz, 1H), 7.11 (d,  $J$  = 7.6 Hz, 1H), 7.04 (s, 1H), 6.87 (t,  $J$  = 7.6 Hz, 1H), 6.81 (d,  $J$  = 7.6 Hz, 1H), 6.75 (d,  $J$  = 8.0 Hz, 1H), 4.00 (br, 4H), 2.00 (m, 4H), 1.05–1.12 (m, 12H), 0.74–0.78 (m, 10H).  $^{13}C\{^1H\}$  NMR (100 MHz, CDCl<sub>3</sub>):  $\delta$  151.6, 151.5, 145.8, 143.4, 142.9, 140.1, 140.0, 139.9, 138.0, 130.5, 129.7, 128.4, 128.2, 127.7, 126.0, 123.6, 121.5, 120.0, 119.8, 118.8, 118.3, 115.7, 114.5, 114.4, 55.2, 40.3, 31.5, 29.7, 23.9, 22.6, 14.0. Calcd for C<sub>37</sub>H<sub>44</sub>N<sub>2</sub>·0.3H<sub>2</sub>O: C, 85.11; H, 8.61; N, 5.36. Found: C, 86.00; H, 8.58; N, 5.42.

**Data of Model-2a.** Yield = 62%.  $^1H$  NMR (400 MHz, CDCl<sub>3</sub>):  $\delta$  7.17 (d,  $J$  = 7.2 Hz, 4H), 6.92 (s, 2H), 6.84 (t,  $J$  = 7.2 Hz, 4H), 6.78 (d,  $J$  = 8.0 Hz, 4H), 3.88 (br, 8H), 1.61 (m, 4H), 1.20 (m, 20H), 0.87 (t,  $J$  = 7.6 Hz, 6H).  $^{13}C\{^1H\}$  NMR (100 MHz, CDCl<sub>3</sub>):  $\delta$  150.4, 144.5, 131.1, 129.2, 128.4, 125.3, 118.5, 117.3, 116.0, 76.7, 70.0, 31.7, 29.3, 29.2, 25.9, 22.6, 14.1. Calcd for C<sub>34</sub>H<sub>48</sub>N<sub>2</sub>O<sub>2</sub>·0.2H<sub>2</sub>O: C, 78.48; H, 9.38; N, 5.38. Found: C, 78.53; H, 8.80; N, 4.99.

**Data of Model-2b.** Yield = 53%.  $^1\text{H}$  NMR (400 MHz,  $\text{CDCl}_3$ ):  $\delta$  7.22 (t,  $J$  = 7.6 Hz, 2H), 7.00 (d,  $J$  = 7.2 Hz, 2H), 6.95 (s, 2H), 6.94 (d,  $J$  = 8.8 Hz, 2H), 6.67 (d,  $J$  = 7.6 Hz, 2H), 3.85 (t,  $J$  = 6.4 Hz, 4H), 3.68 (br, 4H), 1.68 (m, 4H), 1.36 (m, 2H), 1.26 (m, 18H), 0.88 (t,  $J$  = 6.8 Hz, 6H).  $^{13}\text{C}\{^1\text{H}\}$  NMR (100 MHz,  $\text{CDCl}_3$ ):  $\delta$  150.2, 145.2, 139.6, 130.8, 128.8, 120.6, 116.8, 114.2, 70.0, 31.8, 29.37, 29.30, 29.28, 26.1, 22.6, 14.1. Calcd for  $\text{C}_{34}\text{H}_{48}\text{N}_2\text{O}_2 \cdot 0.2\text{H}_2\text{O}$ : C, 78.48; H, 9.38; N, 5.38. Found: C, 78.47; H, 8.71; N, 4.85.

**Synthesis of Model-3.**  $^1\text{H}$  NMR (400 MHz,  $\text{DMSO}-d_6$ ):  $\delta$  9.83 (d,  $J$  = 6.4 Hz, 4H), 9.46 (d,  $J$  = 6.8 Hz, 4H), 8.98 (d,  $J$  = 6.8 Hz, 4H), 8.95 (d,  $J$  = 6.4 Hz, 4H), 8.35 (s, 2H), 8.19 (d,  $J$  = 7.6 Hz, 2H), 8.06 (d,  $J$  = 7.6 Hz, 2H), 8.00 (s, 2H), 7.94–7.89 (m, 6H), 4.76 (q,  $J$  = 7.2 Hz, 4H), 2.17 (s, 4H), 1.63 (t,  $J$  = 7.6 Hz, 6H), 1.00 (s, 12H), 0.68 (t,  $J$  = 6.8 Hz, 6H), 0.58 (s, 4H).  $^{13}\text{C}\{^1\text{H}\}$  NMR (100 MHz,  $\text{DMSO}-d_6$ ):  $\delta$  151.5, 149.3, 148.0, 146.1, 145.7, 142.9, 142.2, 140.4, 137.3, 130.8, 129.6, 126.8, 126.4, 126.3, 123.5, 123.2, 121.5, 120.9, 56.6, 55.3, 30.8, 28.9, 23.5, 21.9, 16.4, 13.8. Calcd for  $\text{C}_{61}\text{H}_{66}\text{Cl}_2\text{I}_2\text{N}_4 \cdot \text{H}_2\text{O}$ : C, 61.16; H, 5.72; N, 4.68. Found: C, 60.89; H, 5.50; N, 4.18.

## References and Notes

- (1) (a) List, E. J. W.; Scherf, U. In *Handbook of Conducting Polymers*, 3rd ed.; Skotheim, T., Reynolds, J., Eds.; CRC Press: New York, 2007; Vol. 1, Chapter 5. (b) Samuel, I. D. W.; Turnbull, G. A. *Chem. Rev.* **2007**, *107*, 1272. (c) Coropceanu, V.; Cornil, J.; Filho, D. A. S.; Olivier, Y.; Silbey, R.; Brédas, J.-L. *Chem. Rev.* **2007**, *107*, 926. (d) Schwab, P. F. H.; Smith, J. R.; Michl, J. *Chem. Rev.* **2005**, *105*, 1197. (e) Watson, M. D.; Fechtenkötter, A.; Müllen, K. *Chem. Rev.* **2001**, *101*, 1267.
- (2) Kovacic, P.; Jones, M. B. *Chem. Rev.* **1987**, *87*, 357.
- (3) (a) Child, A. D.; Reynolds, J. R. *Macromolecules* **1994**, *27*, 1975. (b) Kim, S.; Jackiw, J.; Robinson, E.; Schanze, K. S.; Reynolds, J. R.; Baur, J.; Rubner, M. F.; Boils, D. *Macromolecules* **1998**, *31*, 964–974.
- (4) (a) Kijima, M.; Setoh, K.; Shirakawa, H. *Chem. Lett.* **2000**, 936. (b) Ko, H. C.; Park, S.-A.; Paik, W.-K.; Lee, H. *Synth. Met.* **2002**, *132*, 15.
- (5) Yamaguchi, I.; Shigesue, S.; Sato, M. *React. Funct. Polym.* **2009**, *69*, 91.
- (6) (a) Yue, J.; Gordon, G.; Epstein, A. J. *Polymer* **1992**, *33*, 4410. (b) Chen, S.-A.; Hwang, G.-W. *J. Am. Chem. Soc.* **1995**, *117*, 10055. (c) Chen, S.-A.; Hwang, G.-W. *Macromolecules* **1996**, *29*, 3950. (d) Wei, X.-L.; Wang, Y. Z.; Long, S. M.; Bobeczko, C.; Epstein, A. J. *J. Am. Chem. Soc.* **1996**, *118*, 2545. (e) Breneman, K. R.; Hsu, C.-H.; Shih, H.; Epstein, A. J. *Macromolecules* **2001**, *34*, 2648. (f) Yamamoto, T.; Ushiro, A.; Yamaguchi, I.; Sasaki, S. *Macromolecules* **2003**, *36*, 7075.
- (7) (a) Patli, A. O.; Ikenoue, Y.; Wudl, F.; Heeger, A. J. *J. Am. Chem. Soc.* **1987**, *109*, 1858. (b) Yamamoto, T. *Chem. Lett.* **2003**, *32*, 334. (c) Yamamoto, T. *React. Funct. Polym.* **2003**, *55*, 231.
- (8) (a) Bockstaller, M.; Köhler, W.; Wegner, G.; Fytas, G. *Macromolecules* **2001**, *34*, 6353. (b) Bockstaller, M.; Köhler, W.; Wegner, G.; Vlassopoulos, D.; Fytas, G. *Macromolecules* **2001**, *34*, 6359. (c) Ramey, M. B.; Hiller, J.; Rubner, M. F.; Tan, C.; Schanze, K. S.; Reynolds, J. R. *Macromolecules* **2005**, *38*, 234.
- (9) Zotti, G.; Zecchin, S.; Schiavon, G.; Groenendaal, L. B. *Macromol. Chem. Phys.* **2002**, *203*, 1958.
- (10) (a) Wallow, T. I.; Novak, B. M. *J. Am. Chem. Soc.* **1991**, *113*, 7411. (b) Rau, J. U.; Rehahn, Y. *Polymer* **1993**, *34*, 2889. (c) Chaturvedi, V.; Tanaka, S.; Kaeriyama, K. *Macromolecules* **1993**, *26*, 2607.
- (11) (a) Bäuerle, P.; Gaudi, K. W.; Würthner, F.; Sariciftci, S.; Neugebauer, H.; Hehring, M.; Zhong, G.; Doblhofer, K. *Adv. Mater.* **1990**, *2*, 490. (b) Bartlett, P. N.; Dawsou, D. H. *J. Mater. Chem.* **1994**, *4*, 1805. (c) Kim, B.; Chen, L.; Gong, J.; Osada, Y. *Macromolecules* **1999**, *32*, 3964.
- (12) (a) Peng, Z.; Xu, B.; Zhang, J.; Pan, Y. *Chem. Commun.* **1999**, 1855. (b) Van Severen, I.; Motmans, F.; Lutsen, L.; Cleij, T. J.; Vanderzande, D. *Polymer* **2005**, *46*, 5466.
- (13) (a) Weder, C.; Wrigton, M. S. *Macromolecules* **1996**, *29*, 5157. (b) Yang, J. S.; Swager, T. M. *J. Am. Chem. Soc.* **1998**, *120*, 11864. (c) Wosnik, J. H.; Mello, C. M.; Swager, T. M. *J. Am. Chem. Soc.* **2005**, *127*, 3400.
- (14) (a) Yamamoto, T.; Kimura, T. *Macromolecules* **1998**, *31*, 2683. (b) Yamamoto, T.; Kimura, T.; Shiraishi, K. *Macromolecules* **1999**, *32*, 8886.
- (15) (a) Hayashi, H.; Yamamoto, T. *Macromolecules* **1998**, *31*, 6063. (b) Li, Y.; Vamvounis, G.; Yu, J.; Holdcroft, S. *Macromolecules* **2001**, *34*, 3130. (c) Koren, A. B.; Curtis, M. D.; Francis, A. H.; Kampf, J. W. *J. Am. Chem. Soc.* **2003**, *125*, 5040. (d) Paganin, L.; Lanzi, M.; Costa-Bizzarri, P.; Bertinelli, F.; Masi, C. *Macromol. Symp.* **2004**, *218*, 11.
- (16) Yamaguchi, I.; Choi, B.-J.; Koizumi, T.; Kubota, K.; Yamamoto, T. *Macromolecules* **2007**, *40*, 438.
- (17) (a) Zincke, T. H.; Heuser, G.; Möller, W. *Justus Liebig's Ann. Chem.* **1904**, 333, 296. (b) Marvell, E. N.; Caple, G.; Shahidi, I. *J. Am. Chem. Soc.* **1970**, *92*, 5641. (c) Marvell, E. N.; Shahidi, I. *J. Am. Chem. Soc.* **1970**, *92*, 5646. (d) Kunugi, S.; Okubo, T.; Ise, N. *J. Am. Chem. Soc.* **1976**, *98*, 2282. (e) Eda, M.; Kurth, M. J.; Nantz, M. H. *J. Org. Chem.* **2000**, *65*, 5131. (f) Viana, G. H. R.; Santos, I. C.; Alves, R. B.; Gil, L.; Marazano, C.; Gil, R. P. F. *Tetrahedron Lett.* **2005**, *46*, 7773.
- (18) Yamaguchi, I.; Higashi, H.; Shigesue, S.; Shingai, S.; Sato, M. *Tetrahedron Lett.* **2007**, *48*, 7778.
- (19) (a) Zhou, Q.; Swager, T. M. *J. Am. Chem. Soc.* **1995**, *117*, 12593. (b) Yang, J.-S.; Swager, T. M. *J. Am. Chem. Soc.* **1998**, *120*, 11864. (c) Chen, L.; McBranch, D. W.; Wang, H.-L.; Helgeson, R.; Wudl, F.; Whitten, D. G. *Proc. Natl. Acad. Sci. U.S.A.* **1999**, *96*, 12287. (d) Gaylord, B. S.; Heeger, A. J.; Bazan, G. C. *Proc. Natl. Acad. Sci. U.S.A.* **2002**, *99*, 10954. (e) Pinto, M. R.; Schanze, K. S. *Proc. Natl. Acad. Sci. U.S.A.* **2004**, 7505. (f) Dore, K.; Dubus, S.; Ho, H. A.; Levesque, I.; Brunette, M.; Corbeil, G.; Boissinot, M.; Boivin, G.; Bergeron, M. G.; Boudreau, D.; Leclerc, M. *J. Am. Chem. Soc.* **2004**, *126*, 4240.
- (20) Fuoss, R. M.; Strauss, U. P. *J. Polym. Sci.* **1948**, *3*, 246.
- (21) Dai, S.; Sigman, M. E.; Burch, E. L. *Chem. Mater.* **1995**, *7*, 2054.
- (22) (a) Haskins-Glusac, K.; Pinto, M. R.; Tan, C.; Schanze, K. S. *J. Am. Chem. Soc.* **2004**, *126*, 14964. (b) Dalavi-Malhotra, J.; Chen, L. *J. Phys. Chem. B* **2005**, *109*, 3873. (c) Cabarcos, E. L.; Carter, S. A. *Macromolecules* **2005**, *38*, 10537. (d) Jiang, H.; Zhao, X.; Schanze, K. S. *Langmuir* **2006**, *22*, 5541–5543. (e) Cabarcos, E. L.; Retama, J. R.; Sholin, V.; Cater, S. A. *Polym. Int.* **2007**, *56*, 588.
- (23) Oda, M.; Nothofer, H.-G.; Scherf, U.; Sunjic, V.; Richter, D.; Regenstein, W.; Neher, D. *Macromolecules* **2002**, *35*, 6792.
- (24) Yamamoto, T.; Wataru, I.; Kanbara, T.; Nakamura, Y.; Kikuchi, M.; Ando, I. *Chem. Lett.* **1992**, 2001.
- (25) Yamamoto, T.; Morita, A.; Miyazaki, Y.; Maruyama, T.; Wakayama, H.; Zhou, Z.-h.; Nakamura, Y.; Kanbara, T.; Sasaki, S.; Kubota, K. *Macromolecules* **1992**, *25*, 1214.
- (26) Lightowler, S.; Hird, M. *Chem. Mater.* **2004**, *16*, 3963.